

Repeated use of supported $\text{H}_3\text{PW}_{12}\text{O}_{40}$ catalysts in the liquid phase esterification of acetic acid with butanol

J.H. Sepúlveda*, J.C. Yori, C.R. Vera

*Instituto de Investigaciones en Catálisis y Petroquímica, INCAPE-(FIQ-UNL, CONICET),
Santiago del Estero 2654, 3000 Santa Fe, Argentina*

Received 17 January 2005; received in revised form 18 March 2005; accepted 19 March 2005
Available online 23 May 2005

Abstract

Tungstophosphoric acid (HPA) catalysts supported over SiO_2 , ZrO_2 and carbon were prepared and characterized. Its repeated use in the liquid phase reaction of esterification of acetic acid with butanol was particularly studied. The results revealed that silica- and zirconia-supported HPA had an intrinsic activity per unit protonic acid site greater than that of an Amberlyst W35 resin. Its repeated use was, however, impeded because of the dissolution of HPA in the reaction medium. Carbon-supported HPA catalysts had a slightly lower activity but they displayed a sustained conversion level upon reuse in subsequent catalytic tests. Inspection of the solvent media after the reaction in a UV–visible spectrophotometer revealed that both butanol and water leached HPA from the silica- and zirconia-supported catalysts and that the effect was minimal in the case of the carbon catalysts. It was rationalized that $[\text{PW}_{12}\text{O}_{40}]^{3-}$ anions are strongly adsorbed at pH 1–2 on the carbon support due to the electrostatic interaction with the carbon surface protons of zero-point-of-charge (ZPC) equal to 6.

© 2005 Elsevier B.V. All rights reserved.

Keywords: Supported heteropolyacids; Esterification; Reuse

1. Introduction

Water is present as a reactant in all hydrolysis reactions and as a product in many esterification reactions. Other polar compounds such as alcohols and ketones are also present in the reaction medium as solvents or reactives. These reactions are usually catalyzed by strong liquid acids that are dissolved in the polar reaction media, like sulfuric or fluorhydric acid [1]. These acids are very corrosive and not only pose problems for the design and construction of reactors, buffer vessels and piping systems which must be made of expensive alloys but also arise concern because of their toxicity and environmental impact. Either costly effluent neutralization facilities are set up or they are eliminated untreated with short- and long-term damage to the environment. These problems have motivated a growing interest of researchers in the industrial field and in academic institutions for the replacement of these harmful acids by

solid acid catalysts which not only are environmental friendly materials but also can be repeatedly used in fixed-bed or slurry reactors with easy separation from the products, reactants and solvents, and with sustained activity and selectivity [2,3]. Finding solid acid materials on which the adsorption of heteropolyanions is completely irreversible has been posed as an issue of special interest [4].

Recent reports show that heteropolyacids and heteropolyanions (HPA), like $\text{H}_3\text{PW}_{12}\text{O}_{40}$, are efficient “super-acid” catalysts which can be used both in the homogenous or heterogenous phase [5]: (i) pure HPA solids can be dissolved in many reaction media and (ii) HPA supported over carriers like silica, carbon or transition metal oxides are active catalysts in many acid-catalyzed reactions.

The use of HPA supported over silica, zirconia and carbon, as solid catalysts for the esterification of acetic acid with butanol was studied in this work. The performance of the HPA catalysts was compared against known classical catalysts: acidic resins and sulfuric acid. The repeated use of the HPA catalysts in consecutive batch reaction tests was particularly assessed.

* Corresponding author. Tel.: +54 342 4533858; fax: +54 342 4531068.
E-mail address: jsepulve@fiqus.unl.edu.ar (J.H. Sepúlveda).

2. Experimental

Tungstophosphoric acid, $\text{H}_3\text{PW}_{12}\text{O}_{40}\cdot 6\text{H}_2\text{O}$ (HPA, 99.9%), was supplied by Merck. An acidic sulfonated polymer resin, Amberlyst W35 (1/16" beads, divinyl benzene–styrene) was provided by Rohm and Haas. Amorphous silica–alumina (ASA, Si/Al ratio = 11.3) was provided by Ketjen (LA-LPV type). ZSM-5 zeolite (Si/Al ratio = 20) in the H form was supplied by Chimie Uetikon.

The supports used in the preparation of supported HPA were silica gel (SiO_2 , Grace G-62), activated carbon (AC, Westvaco Nuchar, phosphoric acid-treated, wood base) and zirconia (ZrO_2). ZrO_2 was synthesized from $\text{ZrOCl}_2\cdot 8\text{H}_2\text{O}$ (Strem Chem, 99.998%) by first hydrolyzing the salt in distilled water and then precipitating hydrous zirconia gel by dropwise addition of NH_4OH (Merck, 33%). The precipitate was filtered and washed until no dissolved chloride ions were detected in the washing water by the AgNO_3 test. A $\text{Zr}(\text{OH})_4$ xerogel was obtained by drying the gel at 110 °C. ZrO_2 was finally obtained by calcining $\text{Zr}(\text{OH})_4$ in flowing air ($8\text{ ml min}^{-1}\text{ g}^{-1}$) for 3 h at 500 °C. An acid-treated batch of AC, named here as AC^{at} , was prepared by attacking AC with a diluted aqua regia solution. The AC granules were immersed in the solution (16.6 ml g^{-1}) for 3 h, then they were rinsed with distilled water several times, filtered and dried overnight at 110 °C. ZrO_2 , SiO_2 , AC and AC^{at} were all finally ground in an agata mortar and sieved to 35–80 meshes.

In order to prepare supported HPA, HPA was first dissolved in a diluted HCl solution of pH 1–2, which was prepared by adding drops of concentrated HCl (Merck, 37%) to distilled water. The grafting procedure consisted in dipping the solids (SiO_2 , ZrO_2 , AC and AC^{at}) in the solution (12.5 ml solution per gram of solid) and gently stirring for 3 h at room temperature [6]. Additional experiments were performed in order to assess the adsorption of HPA on virgin carbon (AC) as a function of time and at two different values of pH 1.6 and 3.5. The content on the solid samples was calculated from the content in solution by a mass balance. The liquid was frequently sampled all throughout the experiment, which had a time span of 2 days.

The HPA content in the final catalysts was determined by means of atomic absorption while the content of HPA in solution was determined by UV–visible spectroscopy with the aid of calibration curves. The textural properties of the solid (specific surface area, pore volume and pore size distribution) were measured in a Quantachrome NOVA-1000 sorptometer by physisorption of N_2 at the temperature of $-195.6\text{ }^\circ\text{C}$.

Supported HPA was further characterized by infrared absorption and X-ray diffraction. XRD measurements were performed in a Shimadzu XD-1 diffractometer with $\text{Cu K}\alpha$ radiation filtered with Ni. Spectra were recorded in the 20° – 65° 2θ range and the scanning rate was $1.2^\circ\text{ min}^{-1}$. FTIR spectra of the degassed samples of supported HPA were

taken at room temperature in a Shimadzu FTIR-8101 spectrophotometer, in the range 4800 – 400 cm^{-1} and with a resolution of 4 cm^{-1} . Self-supported wafers were outgassed at 10^{-6} Torr at 100 °C for 1 h before recording each spectrum.

Temperature-programmed decomposition (TPD) tests were also performed. The samples were pretreated in situ by heating in Ar at 100 °C for 1 h before each test. Then, they were heated from 100 to 900 °C at a heating rate of $20\text{ }^\circ\text{C min}^{-1}$ while keeping a flowing stream of He over the sample (20 ml min^{-1}). The evolved species were analyzed on-line with a quadrupole mass spectrometer (Balzers QMS 421). Masses analysed were: $m/e = 44$ (CO_2), $m/e = 28$ (CO), $m/e = 16$ (CH_4), $m/e = 18$ (H_2O) and $m/e = 2$ (H_2).

Fast potentiometric titrations (FPT) were used to measure the polarizability of the surface groups of the samples involved in aqueous acid/base equilibria. A modified version of a previously reported method [7] was used. 0.1 M KNO_3 was used as electrolyte and $\text{HNO}_3/\text{KNO}_3$ and KOH/KNO_3 as titrating solutions. Fifty microlitres of electrolyte were put in a closed vessel and gently stirred under nitrogen bubbling (4 ml min^{-1}) in order to remove dissolved CO_2 . The pH was then adjusted to 7. The sample in the form of a powder (500 mg, ground and sieved to >200 meshes) was then suspended in the solution and a first value of pH was recorded after the pH reading of a glass electrode became stable (± 0.01 in 5 min). Then, the titrating solution (acid or base) was added dropwise. After stabilization, both pH values and amount of added solution were taken down. Traces of the surface charge (σ , $\mu\text{C m}^{-2}$) as a function of pH were obtained from the balance of OH^- and H^+ species in solution and Faraday's conversion of adsorbed ionic species into the corresponding Coulombic charge [7]. Values of the zero-point-of-charge (ZPC) were obtained from the intersection of the σ trace with the pH axis.

Esterification reaction tests were performed in the liquid phase in a stirred tank reactor operated in batchwise mode.

Homogenous reaction: A reacting mixture of acetic acid/butanol/toluene (solvent) with a volume proportion of 25 ml/45 ml/25 ml was first introduced in the reactor. Then the catalyst was introduced: (i) 0.22 g of pure HPA and (ii) 0.22 g of H_2SO_4 .

Heterogenous reaction: A similar reacting mixture of acetic acid/butanol/toluene (solvent) with a volume proportion of 25 ml/45 ml/25 ml was introduced in the reactor. Then the catalyst was introduced: (i) 1 g of HPA/ ZrO_2 ; (ii) 1 g of HPA/ SiO_2 ; (iii) 1 g of HPA/AC; (iv) 1 g of HPA/ AC^{at} and (v) 1 g of Amberlyst resin. Then the temperature was rapidly raised to the desired value, which was varied between 20 and 80 °C. The products of the reaction were analyzed off-site in a HP5890 gas chromatograph equipped with a flame ionization detector and a Supelcowax 10 capillary column (30 m, 0.53 mm i.d., 1 μm film thickness).

3. Results and discussion

3.1. Identification and characterization of HPA species

The results of the atomic absorption and the nitrogen adsorption measurements are included in Table 1. The supported HPA catalysts had HPA contents that varied between 27 and 33%. The activated carbons AC and AC^{at} displayed the highest values of specific surface area, about 1600 m² g⁻¹. The acid treatment produced a small decrease of the specific surface area, likely due to the acid leaching of some non-graphitic, loosely bound carbon atoms, which resulted in a small widening of the pores. The ZSM-5 and ASA samples displayed the second highest values (560–365 m² g⁻¹). ZrO₂ and HPA had the smallest surface area values (6–59 m² g⁻¹). HPA loading produced a decrease of the accessible area of the supports. The effect was mild in the case of the ZrO₂ (36% decrease) and the SiO₂ (24% decrease) samples while it was drastic in the case of the activated carbons (76% decrease). This effect was attributed to the pore plugging of pore channels of the support, supposed to be more extensive in the case of mainly microporous activated carbons.

The XRD spectrum of the commercial HPA sample displayed the peaks of the crystalline state of this acid and they coincided with those previously reported [8]. In contrast, the samples of supported HPA showed no diffraction pattern, indicating that the HPA species were highly dispersed or that the deposited amount of HPA was not big enough to be detected by this technique. The HPA-supported species were, however, detected during the FTIR absorption experiments. The Keggin structure of HPA was confirmed by FTIR spectroscopy. These samples displayed four bands located between 800 and 1110 cm⁻¹ which were attributed to the absorption modes of the Keggin primary structure of the [PW₁₂O₄₀]³⁻. The peaks at 1080, 985, 893 and 812 cm⁻¹ were attributed to the four stretching modes of the oxygen atoms bonded to tungsten and phosphorus which have been assigned to $\nu(\text{P-O})$; $\nu(\text{W=O})$ and $\nu(\text{W-O-W})_{\text{edge}}$ and $\nu(\text{W-O-W})_{\text{corner}}$, respectively [8]. The FTIR spectra of

Table 1
HPA contents as determined by atomic absorption

Samples	S_g (m ² g ⁻¹)	HPA (%)
AC	1621	0.0
AC ^{at}	1562	0.0
SiO ₂	266	0.0
ZrO ₂	59	0.0
W35	45	0.0
ZSM-5	365	0.0
ASA	560	0.0
HPA	6	100.0
HPA/AC	390	33.0
HPA/AC ^{at}	368	29.0
HPA/SiO ₂	203	27
HPA/ZrO ₂	38	29

Specific surface area (S_g) as determined by N₂ sorptometry.

Table 2

Catalytic activity in the liquid phase, homogenous reaction of esterification of acetic acid with butanol ($W_{\text{cat}} = 0.22$ g, $C_B/C_A = 1.1$ and $C_A = 7.14$ mmol ml⁻¹)^a

Catalyst	Temperature (°C)	k (ml mol ⁻¹ h ⁻¹)	k^* (k/meq H ⁺)
HPA	25	1.9	8.8
	40	2.6	11.5
H ₂ SO ₄	25	1.9	0.43
	40	3.0	0.70

Observed kinetic constant (k) and specific kinetic constant (k^*).

^a The number of protons of H₂SO₄ in solution was calculated by assuming total ionization. The number of protons of HPA was determined by assuming total dissolution (3 protons per molecule).

the supported HPA samples were all very similar and were used for the identification of the Keggin structure only. Quantification was more amenable in the case of the UV-spectra (Section 3.3.2) and for this reason the FTIR spectra are not included.

3.2. Catalytic activity results

3.2.1. Homogenous reaction

The activity of dissolved HPA was compared to that of dissolved H₂SO₄ (Merck, 98%). It was assumed that the esterification reaction proceeds with a second-order reaction rate [9]:

$$r_A = kC_A C_B \quad (1)$$

where k is the observed kinetic reaction rate and has units of ml mol⁻¹ h⁻¹. A mathematical relation between the reaction time (t), the conversion of acetic acid (X_A), the initial concentration of acetic acid (C_A) and the initial concentration of butanol (C_B) can be found by integrating equation (1), after considering a perfectly mixed phase inside the reactor volume:

$$Ckt = \frac{1}{1-M} \ln \frac{M(1-X_A)}{M-X_A} \quad (2)$$

$$M = \frac{C_{A0}}{C_{B0}} \quad (3)$$

$$X_A = \frac{C_{A0} - C_A}{C_A} \quad (4)$$

A good degree of correlation ($r^2 = 0.99$) was obtained when a least squares fit was tried between the experimental values and equation (2). Worse degrees of correlation ($r^2 < 0.95$) were obtained when zero-order or first-order kinetic models were adopted.

Table 2 contains the values of the kinetic constant k obtained using a linear regression program for fitting the experimental values with equation (2). It can be seen that HPA is more active than H₂SO₄, either when the global, observed kinetic constants k , or when the specific constants k^* , are compared. k^* is the kinetic constant normalized by dividing k by the number of acid protons of the catalyst.

The results agree with previous ones reported elsewhere which indicate that HPA is more active than H_2SO_4 in a wide variety of acid-catalyzed reactions [10,11].

3.2.2. Heterogenous reaction

The test reaction was catalyzed with the supported HPA catalysts and other standard catalysts for comparison, the W35 resin, ASA and the ZSM-5 zeolite. The results of Table 3 show that the specific activity (k^*) of the fresh HPA/ SiO_2 and HPA/ ZrO_2 catalysts is higher than that of the bulk HPA catalyst (see Table 2). We can see that supporting HPA over an activated carbon produces a decrease of the specific activity as compared to the other supported HPA catalysts.

The global reaction rate follows a different order depending on the temperature, although HPA/ SiO_2 is always the most active catalyst.

$\text{HPA}/\text{SiO}_2 > \text{HPA}/\text{ZrO}_2 > \text{HPA}/\text{AC} > \text{W35} > \text{ASA}$,
 $T = 40^\circ\text{C}$

$\text{HPA}/\text{SiO}_2 > \text{W35} > \text{HPA}/\text{ZrO}_2 > \text{HPA}/\text{AC} > \text{ZSM} - 5$,
 $T = 60^\circ\text{C}$

The activity per unit protonic site follows a unique order irrespective of the temperature:

$\text{HPA}/\text{SiO}_2 > \text{HPA}/\text{ZrO}_2 > \text{HPA}/\text{AC} > \text{W35}$,
 $T = 40\text{--}60^\circ\text{C}$

The W35 resin has only Brönsted acid sites and these sites have an acid strength higher than that of H_2SO_4 protons [12], i.e. W35 can be called a “superacid” [13]. For this reason is a commercial catalyst for acid-catalyzed reactions and is interesting to compare its catalytic performance with HPA [14] and its supported counterparts being studied. The results of Table 3 indicate that the least active supported HPA catalyst, HPA/AC, has a specific activity one order of magnitude higher than W35. With HPA/AC

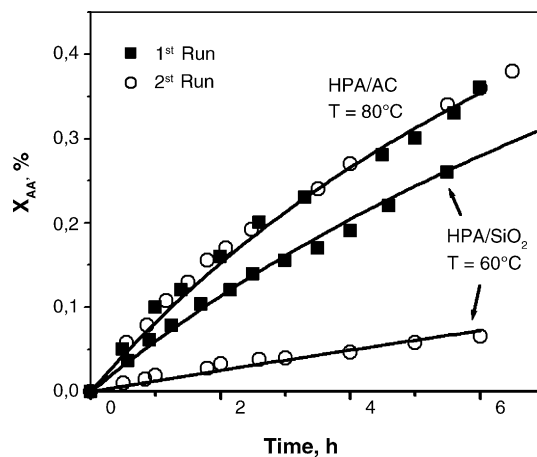


Fig. 1. Conversion of acetic acid (X_{AA}) as a function of time on supported HPA catalysts in consecutive reaction tests. (□) First batch, 60°C and (△) second batch, 60°C . (■) First batch, 80°C and (▲) second batch, 80°C .

and at temperatures of $60\text{--}80^\circ\text{C}$, conversion values near the thermodynamic equilibrium (66% conversion) were obtained after 8 h of time of reaction.

3.3. Stability

3.3.1. Consecutive catalytic tests

After the first catalytic test (time of reaction = 8 h), the catalysts were filtered and used in a second test. The procedure was repeated in a third reaction test. Fig. 1 contains the plots of the conversion of acetic acid as a function of the reaction time and Table 4 contains the values of the global kinetic constants during the first and second test. It can be seen that the activity of the HPA/ SiO_2 and HPA/ ZrO_2 catalysts drops to almost negligible values after being used in the first batch. A change in the value of the k^* specific constant is not likely and, therefore, we suppose that a great portion of the active material, HPA, was leached during the reaction and was

Table 3

Catalytic activity of acid catalysts in the reaction of esterification of acetic acid with butanol ($W_{\text{cat}} = 1\text{ g}$, $C_{\text{B}}/C_{\text{A}} = 1.1$ and $C_{\text{A}} = 7.14\text{ mmol ml}^{-1}$)

Catalyst	Temperature ($^\circ\text{C}$)	k ($\text{ml mol}^{-1}\text{ h}^{-1}$)	k^* (k/meq H^+)	E_a (kcal mol^{-1})
W35	40	2.5	0.5 ^b	16.3
	60	10.8	2.0	
HPA/AC	40	2.9	10.0	11.3
	60	5.8	20.1	
HPA/ SiO_2	40	6.2	23.8	10.6
	60	13.0	56.2	
HPA/ ZrO_2	40	5.2	22.5	10.2
	60	7.1	45.3	
ASA	40	0.13	0.12 ^a	23.8
	60	1.3	1.2 ^a	
ZSM-5	40	0.9	1.82 ^a	6.6
	60	1.4	1.82 ^a	

Observed kinetic constant (k), specific kinetic constant (k^*) and activation energy (E_a).

^a From TPD of trimethylpyridine.

^b $[\text{H}^+] = 5.4\text{ meq/g}$.

Table 4
Repeated use of HPA-supported catalysts

Samples	k (ml mol ⁻¹ h ⁻¹)		
	First batch, fresh catalyst	Second batch, used catalyst	Third batch, used catalyst
HPA/AC	5.8	5.6	5.5
HPA/AC ^{at}	6.3	4.3	2.8
HPA/SiO ₂	13.0	1.7	—
HPA/ZrO ₂	7.1	1.4	—

Catalytic activity in consecutive tests; observed kinetic rate; reaction conditions: 60 °C, $W_{\text{cat}} = 1$ g, $C_B/C_A = 1.1$ and $C_A = 7.14$ mmol ml⁻¹.

discarded during filtering. The leaching occurs because the heteropolyanion has a greater affinity for the solvent medium than for the surface of the support. In other words, the heat of solvation is greater than the heat of adsorption. In the case of the HPA/AC catalyst, the dissolution in the solvent is seemingly minimal because the activity loss between different batches is small. HPA is, therefore, strongly adsorbed over carbon in the reaction conditions while it is only weakly adsorbed over silica and zirconia.

3.3.2. UV–visible spectroscopy results

The pH of the solution plays a very important role as it governs the apparent stability constants of the species which are in equilibrium. According to Pizzio et al. [15], H₃PW₁₂O₄₀ has a Keggin structure stable at acid pH values lower than 2. According to Jansen et al. [16], the stability occurs at pH values lower than 5.5. Table 5 contains the position of the maxima of the UV–vis spectra of the HPA dissolved in water. The spectrum is the same for pH values between 1 and 4. However, at pH 5, an 8 nm shift can be detected, indicating the presence of the species [PW₁₁O₃₉]⁷⁻. In order to verify the dissolution of HPA supported on SiO₂, ZrO₂ and activated carbon, solid samples of HPA/SiO₂, HPA/ZrO₂, HPA/AC^{at} and HPA/AC were collected and dipped in butanol and water. Inspection of the UV–vis spectra of the liquid phase enabled the detection of HPA both in butanol (band at 266.6 nm) and water (band at 260 nm [17]) in the case of the HPA/SiO₂ and HPA/ZrO₂ catalysts (see Fig. 2). No HPA bands were detected in the case of the HPA/AC catalyst. In the case of the HPA/AC^{at} catalyst, the acid treatment lowers the ZPC of the carbon to 2.0, a value very near the pH of the HPA solution, 1.6. Since the pH is almost at the ZPC point, the surface charge is extremely low and the HPA species are poorly adsorbed at the surface because there is negligible electrostatic attraction. Most HPA remains in solution and for this reason, the content of HPA in solution in the case of the HPA/AC^{at} sample is almost the highest.

Table 5
Analysis of the reaction medium after the reaction at different pH values

pH	λ (nm)
1	264.0
2	264.1
3.5	264.0
4	264.0
5	256.0

Wavelength of the peak of maximum absorbance.

3.3.3. Physical properties of HPA/AC

Pore size distribution data are presented in Fig. 3. Virgin-activated carbon has a monomodal distribution with a maximum located at 22 Å. The acid treatment practically does not affect the total pore volume or the area. A small fraction of the micropore volume is lost, but the effect is negligible. The adsorption of HPA produces a high and uniform decrease of the pore volume all throughout the pore diameter range, with no special effects in the micropore or mesopore regions.

These results indicate that no differences in HPA adsorption related to different textural properties can be expected because the texture of AC and AC^{at} are almost equal and the HPA adsorption affects equally all domains of the pore structure, regardless of their pore size.

The strong adsorption of HPA over carbon can be due to the porous structure of the carbon because the HPA particles can be trapped inside its small pores. Another possibility is that the strong adsorption arises from the existence of specific groups on the surface of the carbon that produce a strong electrostatic attraction of the HPA species. The second case is the most probable. AC^{at} is a support that was produced by chemically attacking the virgin-activated carbon with a strong mineral acid. AC^{at} and AC had similar textural properties (results in Table 1 and Fig. 3) but they generated HPA-supported catalysts of very different stability. The HPA supported over AC^{at} was dissolved in the reaction medium while that supported over AC was not (recall the results of Fig. 2).

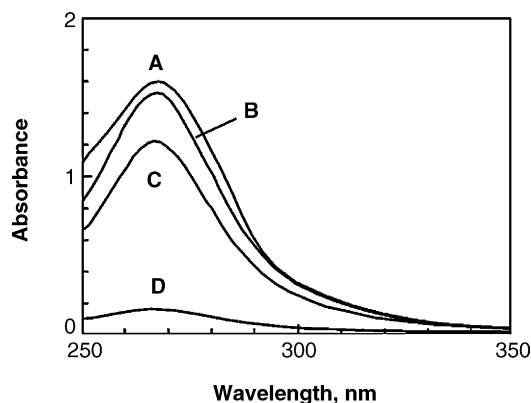


Fig. 2. UV–vis absorbance spectra of the solution (butanol) after being in contact with HPA-supported catalysts (curve A, HPA/SiO₂; B, HPA/AC^{at}; C, HPA/ZrO₂ and D, HPA/AC).

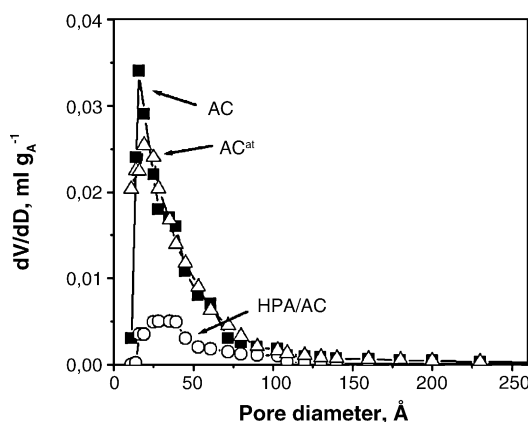


Fig. 3. Pore size distributions of the HPA/AC, AC and AC^{at} samples.

3.3.4. Potentiometric titration of HPA/AC

The knowledge of the polarizability of the surface and of the ZPC is very important for the preparation of supported catalysts [18]. The precursors of the final supported species must usually be firstly electrostatically adsorbed on the surface and conditions of impregnation must be chosen that ensure that the precursor in solution, usually an anion or a cation, is correctly attracted to the surface of the support. pH conditions and choice of precursor must be fine tuned in order to meet several requirements: (i) if the surface is negatively charged, the precursor in solution must be a cation; (ii) if the surface is positively charged, the precursor in solution must be an anion; (iii) during the preparation, the pH of the medium is such that the polymerization degree of the precursor is sufficiently small in order to prevent pore plugging and transport limitations and (iv) solvation forces do not overcome adsorption forces.

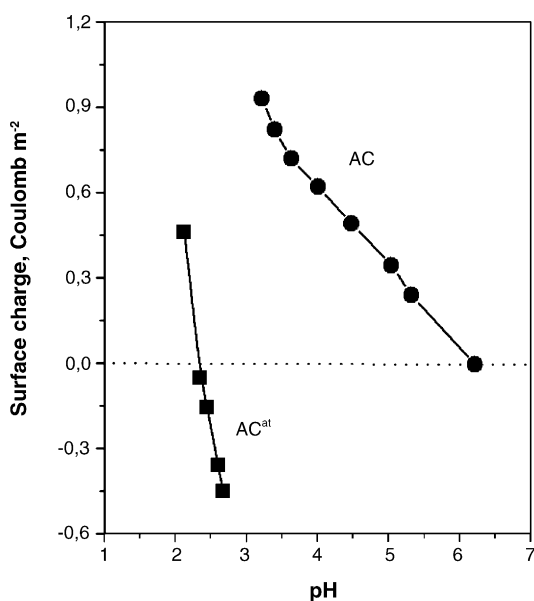
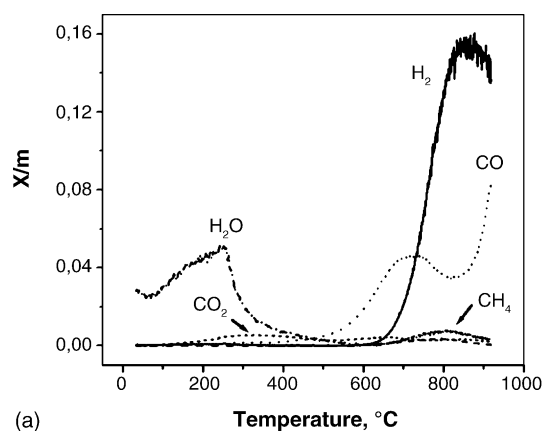
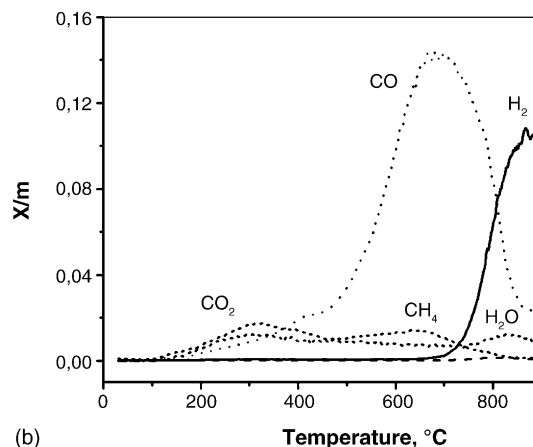


Fig. 4. Fast potentiometric titration curves of the virgin and acid-treated activated carbons.



(a)



(b)

Fig. 5. Results of temperature-programmed decomposition with mass-spec detection: (a) HPA/AC catalyst and (b) HPA/AC^{at} catalyst.

The ZPC values reported in the open literature vary widely from 1 to 10 pH units. This is due to the great variety of raw materials that activated carbons are made from (lignite, coconut shells, wood, etc.) and the different activation treatments used in the industry (with acids, alkalis, steam, CO₂, etc.). Many authors [19,20] agree that oxidizing treatments with mineral acids, e.g. aqua regia, produce a negative shift of the ZPC because of the formation of surface groups containing oxygen, which is an atom more electronegative than carbon. The results of Fig. 4 indicate that AC^{at} has a ZPC = 2 and that virgin AC had a ZPC = 6.

3.3.5. Temperature-programmed decomposition of HPA/AC

The activated carbons were further characterized by temperature-programmed decomposition in an inert atmosphere. The carbons were heat treated from 100 °C to temperatures as high as 900 °C. Fig. 5 shows that the decomposition of AC produces gases with the following order of importance: H₂ > CO ≫ CO₂, CH₄. In contrast, the decomposition of AC^{at} produces gases in different relative amounts: CO ≫ H₂ ≫ CO₂, CH₄. These results indicate that the surface of AC^{at} has a greater concentration of oxygen than the surface of AC. If we integrate the curves to

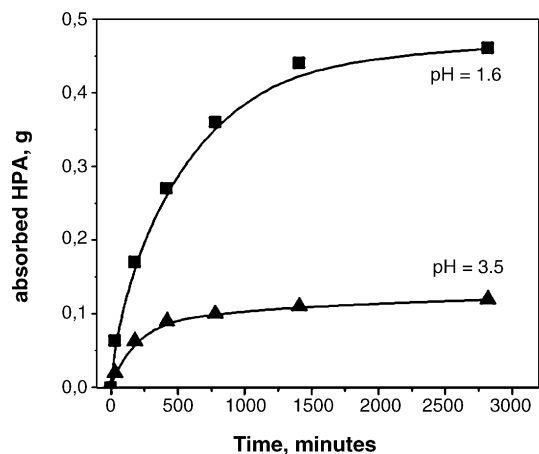


Fig. 6. Adsorption as a function of time of HPA over virgin-activated carbon (■) pH 1.6 and (▲) pH 3.5.

obtain an estimate of the total amount of evolved gases and make a ratio between the values for the two carbons, the results indicate: $\text{CO}_2^{\text{at}}/\text{CO}_2^{\text{virgin}} = 2.6$, $\text{CO}^{\text{at}}/\text{CO}^{\text{virgin}} = 2.6$ and $\text{H}_2\text{O}^{\text{at}}/\text{H}_2\text{O}^{\text{virgin}} = 0.52$. The amount of surface oxygen is, therefore, approximately increased 160% by the oxidizing treatment with mineral acid while the amount of surface H atoms are depleted by 50%.

We can, therefore, conclude that the surface of the activated carbon can be modified by oxidizing it with mineral acids and in this way the polarizability and the strength of the adsorption of the HPA can be modulated.

3.3.6. Effect of the pH on the adsorption of HPA

Results of adsorption of HPA as a function of time and at two different values of pH are plotted in Fig. 6. In the conditions of both tests, the surface is positively charged because the pH is lower than the ZPC (6.4). According to the FPT curve of AC of Fig. 4, the surface density charge at pH 1.6 is much higher than the density at pH 3.5. As expected, the results of Fig. 6 clearly show that the adsorption capacity of the activated carbon for HPA is increased at lower pH values.

4. Conclusions

Heteropolyacids (HPA) efficiently catalyze the esterification reaction of acetic acid with butanol. In the homogenous phase, dissolved HPA has a specific activity

(per unit proton) greater than the activity of sulfuric acid. HPA supported over silica has the highest specific activity but it gets dissolved in the reaction medium; the same happens with the zirconia-supported HPA catalyst. Both cannot be used to process successive batches of reactants in discontinuous systems.

HPA supported over activated carbon is strongly adsorbed on the surface and does not dissolve during the reaction. This catalyst has a good conversion level and can be repeatedly recovered and used in batchwise discontinuous systems.

The strong grafting of the heteropolyanion on the carbon surface is not due to the trapping of anions in small pores but to a strong electrostatic adsorption due to the high density of positive charge developed by the surface groups of the carbon at pH values lower than 6.

References

- [1] K. Urabe, M. Ogawa, Y. Izumi, *Appl. Catal.* A32 (1995) 127.
- [2] S. Soled, S. Misco, G. McVicker, W.E. Gates, A. Gutierrez, J. Paes, *Chem. Eng. J.* 64 (1996) 247.
- [3] T. Kengaku, Y. Matsumoto, K. Na, M. Misono, *J. Mol. Catal. A: Chem.* 134 (1998) 237.
- [4] S.R. Mukai, T. Sugiyama, H. Tamon, *Appl. Catal. A* 256 (2003) 99.
- [5] N. Mizuno, M. Misono, *J. Mol. Catal.* 86 (1994) 319.
- [6] P. Dupont, F. Lefebvre, *J. Mol. Catal. A: Chem.* 114 (1996) 299.
- [7] W. Stumm, J. Morgan, *Aquatic Chemistry*, Wiley Interscience, New York, 1970 (Chapter 4).
- [8] M. Misono, *Catal. Rev. Sci. Eng.* 29 (1987) 269.
- [9] J.B. Moffat, B.K. Hodnett, *J. Catal.* 88 (1984) 253.
- [10] P. Dupont, J. Védrine, E. Paurmard, G. Hecquet, F. Lefebvre, *Appl. Catal. A* 129 (1995) 217.
- [11] I.V. Kozhevnikov, A.S. Matveev, *Appl. Catal.* 5 (1983) 135.
- [12] I.V. Kozhevnikov, A.I. Tsyganok, M.N. Timofeeva, S.M. Kulikov, V.N. Sidelnikov, *React. Kinet. Catal. Lett.* 46 (1992) 17.
- [13] G.A. Olah, G.K.S. Prakash, J. Sommer, *Superacids*, Wiley, New York, 1985.
- [14] Y. Izumi, K. Matsuo, K. Urabe, *J. Mol. Catal.* 18 (1983) 299.
- [15] L.R. Pizzio, C.V. Cáceres, M.N. Blanco, *Appl. Catal. A* 167 (1998) 283.
- [16] R.J.J. Jansen, H.M. van Veldhuizen, M.A. Schwegler, H. van Bekkum, *Recl. Trav. Chim. Pays-Bas* 113 (1994) 115.
- [17] H. Kimura, T. Nakato, T. Okuhara, *Appl. Catal. A* 165 (1997) 227.
- [18] J.P. Brunelle, A. Sugier, J.F. Lepage, *J. Catal.* 43 (1976) 273.
- [19] J.R. Radovic, F. Rodríguez-Reinoso, *Ser. Adv. Chem. Phys. Carbon* 25 (1997) 243.
- [20] M.A. Schwegler, P. Vinke, M. van der Eijk, H. van Bekkum, *Appl. Catal.* 80 (1992) 41.